AIAA JOURNAL
Vol. 36, No. 9, September 1998

Scaling the Near-Field Centerline Mixing Behavior of Axisymmetric Turbulent Jets

George Papadopoulos* and William M. Pitts†
National Institute of Standards and Technology, Gaithersburg, Maryland 20899

Detailed measurements of the centerline mixing behavior in the near field of variable-density jets were performed. Real-time measurements of jet fluid concentration for a propane jet and a methane jet issuing into still air were made utilizing Rayleigh light scattering. The initial conditions were those of fully developed pipe flow, and testing was done for flow rates yielding Reynolds numbers in the range of 3.3×10^3–2.3×10^4, based on the average discharge velocity, exit diameter, and initial fluid properties. Centerline decay characteristics in the near field exhibited a downstream shift with increasing Reynolds number, which was attributed to the initial velocity distribution at the jet exit. Investigation of the mean and turbulent characteristics of the initial velocity distribution yielded a proposed near-field scale variable that effectively captured this dependence on Reynolds number. Collapse of the near-field centerline velocity and concentration distributions was achieved using the proposed scaling.

Nomenclature

A = jet cross-sectional area
F = flatness of velocity distribution
I = Rayleigh light scattering intensity
J = momentum flux, $\int_A \rho U^2(z, r)\, \mathrm{d}A$
K = centerline decay rate
M_0 = initial mass flux component due to velocity distribution, $\int_{A_0} U(0, r)\, \mathrm{d}A$
$\dot{m}$ = mass flux, $\int_A \rho U(z, r)\, \mathrm{d}A$
N_0 = initial momentum flux component due to velocity distribution, $\int_{A_0} U^2(0, r)\, \mathrm{d}A$
Re = Reynolds number, $2\rho_0 U_0 r_0/\mu_0$
R_ρ = density ratio, ρ_0/ρ_∞
r = radial distance, positive outward from jet centerline
r_0 = initial jet radius
r^* = length scale incorporating mass, momentum, and turbulence intensity characteristics
S = skewness of velocity distribution
Tu = turbulence intensity, $U'/\bar{U}$
t = time
U = velocity
X = mole fraction
Y = mass fraction
z = streamwise distance, measured from jet exit and positive in bulk flow direction
z_0 = virtual origin
z^* = nondimensional streamwise distance
κ = exponent to power law velocity distribution
μ = viscosity
ρ = density
τ = turbulence intensity flux per unit area, $\frac{1}{A}\int_A \frac{U'(z, r)}{\bar{U}(z, r)}\, \mathrm{d}A$
$()'$ = rms value
$\bar{()}$ = time-averaged mean value

Subscripts

b = bulk (average)
c = concentration field
m = centerline
u = velocity field
ε = effective
0 = jet exit plane
∞ = ambient (surroundings)

Received Sept. 22, 1997; presented as Paper 98-0695 at the AIAA 36th Aerospace Sciences Meeting and Exhibit, Reno, NV, Jan. 12–15, 1998; revision received May 10, 1998; accepted for publication May 11, 1998.

*Mechanical Engineer, Building and Fire Research Laboratory; currently Applications Engineer, Dantec Measurement Technology, 777 Corporate Drive, Mahwah, NJ 07430. Senior Member AIAA.

†Supervisory Research Chemist, Building and Fire Research Laboratory.

Introduction

AXISYMMETRIC jets have been the subject of continuous research for several decades, and much information on the mixing characteristics of various configurations exists.[1–3] The knowledge obtained from observing this basic flow has been useful in gaining insight into many engineering problems. Circular turbulent jets in particular are involved in many practical systems because of their ability to provide high mixing rates in simple and safe configurations. Information about the near field in these jets is useful as important interacting processes, such as combustion, recirculation, and entrainment, are initiated and conditioned in the early stages of jet development.

Far-field behavior and the attainment of self-similarity has drawn much of the attention focused on jet flows. In spite of this effort, a shortcoming of the available data, often expressed by investigators reviewing the literature,[2,3] has been the lack of well-defined initial conditions. Conditions at the jet exit dominate the early stages of jet development, namely, the growth of the initial mixing layers in the potential core region of the jet and the transition region between the end of the potential core and the downstream location where the jet attains self-similarity. These two regions will be referred to collectively as the near-field region in this paper.

The attainment of self-similar behavior implies no additional influence of initial conditions on the jet behavior. Hence, in looking at the far-field self-similar behavior of jets, it is understandable why investigators have often neglected to fully characterize their initial conditions. The equations used to describe far-field similarity along the centerline for a constant-density axisymmetric jet issuing into still air are

$$\frac{\bar{U}(0, 0)}{\bar{U}(z, 0)} = K_u\left(\frac{z - z_{0,u}}{r_0}\right), \qquad \frac{U'(z, 0)}{\bar{U}(z, 0)} = \text{const} \tag{1}$$

$$\frac{\bar{Y}(0,0)}{\bar{Y}(z,0)} = K_c\left(\frac{z - z_{0,c}}{r_0}\right), \qquad \frac{Y'(z,0)}{\bar{Y}(z,0)} = \text{const} \tag{2}$$

Note that Eqs. (1) and (2) are similar and representative of other scalar quantities as well, but mass fraction is emphasized here because the present paper deals with measurements of mass fraction only and not any other scalar quantity. The terms $z_{0,u}$ and $z_{0,c}$ are the virtual origins. These terms are displacements along the centerline of the jet representing a correction to the actual origin that yields the location where an idealized point jet source, having the same mass, momentum, and far-field development as the actual jet, would be located. They can thus be regarded as a means of incorporating the effects of nonidealized initial conditions. Existing measurements of mean velocity distributions indicate that profiles become self-similar (or self-preserving) some few diameters downstream of the jet exit. The turbulent intensities, however, show marked departures from self-preservation even on the axis of the jet. Based on the latter observation, Townsend[4] concluded that the effect of the initial conditions near the jet exit diminishes rather slowly with downstream distance. Wygnanski and Fiedler[5] considered this effect in their investigation of the self-preserving jet and noted that some 70 diameters may be required for the jet to attain truly self-preserving behavior.

Mass, momentum, and turbulence distributions at the exit plane influence flow development in the near and far (self-similar) fields of the jet. For variable-density jets, Thring and Newby[6] used momentum conservation to show that the influence of the initial density difference on the far-field flow may be accounted for by introducing the concept of an effective radius, $r_\varepsilon = r_0 R_\rho^{1/2}$. Its currently accepted form is

$$r_\varepsilon = \frac{\dot{m}_0}{(\pi \rho_\infty J_0)^{\frac{1}{2}}} \tag{3}$$

and it represents the radius of a hypothetical jet with density ρ_∞ and the same initial mass flux $\dot{m}_0$ and momentum flux J_0 as the jet under consideration. This concept has been used successfully by several researchers to scale concentration field data in the far field of variable-density jets.[7–12] Furthermore, Dahm and Dimotakis[13] show, using dimensional analysis, that the effective radius as defined in Eq. (3) is the proper variable for normalizing the axial coordinate of the jet fluid concentration in the far field. The validity of Eq. (3) is limited to the far field because Eq. (3) requires that the average density of the jet asymptotically approaches the ambient density, a condition that is not valid in the near field where large density gradients exist between the jet core and the ambient.

Richards and Pitts[12] in their investigation of variable-density jets concluded that the final asymptotic state of all momentum-dominated axisymmetric jets depends only on the rate of momentum addition when the streamwise distance is scaled appropriately with r_ε. They show that, regardless of the initial conditions (fully developed pipe and nozzle flow), axisymmetric turbulent free jets decay at the same rate and spread at the same half-angle and that both the mean and rms mass fraction values collapse in a form consistent with full self-preservation. This presentation of jet properties is, however, in relative terms because embodied in the axial scaling is the virtual origin displacement, which, as they note, requires further investigation to understand its dependence on initial jet parameters. Furthermore, they point out that two distinct virtual origins, one associated with the centerline decay and the other with the profile's half-width decay, are necessary to collapse the data in terms of similarity parameters.

Investigations focusing on the variation of the virtual origin have indicated qualitatively how various initial parameters, such as Reynolds number, profile shape, turbulence intensity, and density ratio, affect its location. Some attempts at quantifying the trends observed, especially with respect to Reynolds number, have yielded empirical relations that are merely best fits to specific experimental data (see the discussion by Pitts[14]). These correlations indicate a downstream displacement of z_0 with increasing Reynolds numbers, reaching an asymptotic value for large Reynolds numbers. The conclusion by Pitts[14] was that the physical mechanisms responsible for the Reynolds-number dependence are not understood. He speculated that the downstream shift in the virtual origin with increasing Reynolds numbers for axisymmetric jets having fully turbulent initial conditions is a result of longer flow distances being required at higher Reynolds numbers for achieving the self-similar state in the far field.

Turbulent flow discharging from long straight pipes normally exhibits fully developed conditions at the exit plane. These conditions provide a baseline flow condition (fully developed flow) that is generally understood. Patel[15] indicates that, if the flow in a pipe at some point downstream of the inlet is deemed to be fully developed, then it should hold no memory of its initial development history. He suggests using the local turbulence intensity as an indicator. Then for a fully developed turbulent flow through a pipe, the turbulence intensity at the point of observation remains unchanged as the entry conditions are altered. When the flow entering a smooth pipe is initially tripped and then allowed to develop, fully turbulent conditions exist for $Re \gtrsim 3.5 \times 10^3$ as shown by Papadopoulos and Durst.[16] Under these conditions the shape of the velocity profile does not remain unchanged but appears to approach an asymptotic state as the Reynolds number increases. This behavior is clearly seen in the early work on pipe flow done by Nikuradse.[17] In more recent experiments using laser Doppler velocimetry in a refractive indexed matched facility, Durst et al.[18] measured the velocity profile near the pipe wall and were able to determine directly the shear stress at the wall. They then looked at the accuracy of the law-of-the-wall scaling in the low-Reynolds-number regime past transition and noticed an asymptotic trend. They reported that constant values for the scaling constants were not attained until $Re \approx 1.4 \times 10^4$. Similar asymptotic trends have been observed regarding the virtual origin and potential core length of turbulent axisymmetric jets,[14,19–21] which have been attributed to variations in the initial conditions and have given rise to empirical formulations based on Reynolds numbers.

The similar trend with Reynolds numbers of the velocity profile in fully developed turbulent pipe flow and of the jet's near-field centerline behavior (shift of virtual origin) under these conditions motivated the present authors to attempt to correlate the two behaviors. The exit conditions of a jet formed by fully developed flow discharging from a smooth pipe have been measured for several Reynolds numbers in the range of 3.3×10^3–2.3×10^4 so as to understand the physical mechanisms that couple the two phenomena, with the desire of providing a means for scaling the near-field development of turbulent jets using the initial flow conditions.

Experimental Setup and Methodology

A. Facility

Real-time measurements of jet concentration were made using Rayleigh light scattering (RLS) in the quiescent environment of a cylindrical clean room, dubbed the Rayleigh Light Scattering Facility (RLSF). This facility was carefully designed to minimize interferences associated with glare and Mie scattering due to particles that tend to overwhelm the RLS signal. A detailed description, plus a schematic, of the RLSF may be found in Ref. 22, and only a short overview will be given here.

The RLSF is composed of a 3.0-m-tall × 2.4-m-diam cylindrical test section that is completely isolated from the surrounding laboratory environment during operation, an air distribution system to purge the test section with clean air after each experiment, and high-efficiency particulate filters to remove small particles. Each experiment was initiated by using the blower box unit with the two variable-speed fans to circulate air through the filters and test section for the removal of small particles. The purging continued until the RLS signal, observed on an oscilloscope, showed no signs of Mie scattering. Testing was initiated after shutting down the fans and waiting for flow transients to dissipate, about 30–40 s. After testing, jet gases were purged from the test section by opening the air distribution system to the laboratory exhaust, while makeup air passed through the filters. The total time for each individual test was limited to about 1 min to prevent significant ambient stratification as a result of jet fluid buildup. During this time, sets of three to four RLS point measurements were performed, depending on the data acquisition and jet flow rate conditions.

B. Rayleigh Light Scattering Measurements

The optical system was similar to that described in Ref. 23. The light source was an argon-ion laser operating on all lines at a nominal

power of 20 W. The beam entered the RLSF through a Brewster-angle window and was then focused by a 250-mm-focal-length lens to a narrow waist of 50-μm diam. The receiving optics were positioned perpendicular to the laser beam. The scattered light was collected by an $f/2$ lens system and imaged 1:1 onto a 400-μm pinhole, which defined the length of the observation volume. The intensity of the imaged light was converted to an electrical signal by a Thorn EMI Model 9781B photomultiplier tube (PMT). (Certain commercial equipment, instruments, or materials are identified in this paper to adequately specify the experimental procedure. Such identification does not imply recommendation or endorsement by the National Institute of Standards and Technology, nor does it imply that the materials or equipment are necessarily the best available for the purpose.) The current output of the PMT was fed into a Stanford Research Systems Model SR570 Low-Noise Current Preamplifier. Cutoff frequencies of 3 and 10 kHz were used, thus defining the Nyquist frequency for data sampling. The voltage output of the SR570 was then passed to a 12-bit digitizer interfaced to a Masscomp 5450 computer. For determining the mean concentration statistics, 69,000 points at a sampling speed of 6 kHz were acquired at locations along the centerline of the jet and over the entire field. Additionally, 80,000 points at a sampling speed of 20 kHz were acquired at locations in the near field of the jet. The data were stored on the hard disk for postprocessing.

During each experiment the laser power was also monitored and sampled simultaneously with the RLS signal by measuring laser light reflected off the Brewster-angle window with a photodiode. This allowed minor laser power drifts and fluctuations (1–2%) to be normalized out of the measurements.

Concentration measurements were performed in the manner described by Pitts and Kashiwagi.[23] The RLS intensity was first calibrated by recording the mean scattering intensity of the ambient gas (air in the present case), I_∞, and the jet gas, I_0. The turbulent jet was then initiated, and the real-time RLS signal $I(t)$ was recorded. The mole fraction $X(t)$ was subsequently determined by

$$X(t) = \frac{I(t) - I_\infty}{I_0 - I_\infty} \tag{4}$$

and then converted to mass fraction $Y(t)$

$$Y(t) = \frac{\rho_0 X(t)}{\rho_\infty [1 - X(t)] + \rho_0 X(t)} = \frac{R_\rho X(t)}{1 + [R_\rho - 1]X(t)} \tag{5}$$

The uncertainty in determining the mean mass fraction was estimated to be less than 2%. (Reported uncertainties are at 95% confidence.)

C. Test Configuration and Conditions

Two gases were used in the present investigation—propane and methane—to examine initial density effects on jet development. The density ratios were $R_\rho = 1.521$ and 0.553, respectively. The jet was produced by a long straight pipe, 6.08 ± 0.04 mm i.d., having a sharp-edged exit (wall thickness of less than 0.25 mm). The gas supply to the pipe passed first into a cylindrical settling chamber (120 mm long and 100 mm in diameter) and then through a series of pipe fittings before entering the pipe. The fittings provided the necessary initial artificial disturbance to achieve fully developed turbulent conditions at the exit of the pipe, 103 diameters downstream, for the flow rates considered in the investigation.

The flow assembly was mounted on a three-axis, computer-controlled positioning traverse placed on the floor of the RLSF. Linear encoders mounted along each axis and interfaced to an ACU-RITE III digital readout system provided an absolute measure of position to within ± 0.01 mm. The digital output of the readout system was integrated with the positioning control sequence of each motor, thus greatly reducing motor-travel inaccuracies. The pipe assembly was mounted on the traverse with the gas issuing upward into the RLSF enclosure. The error associated with the initial positioning of the measurement volume with respect to the axis origin centrally located in the jet exit plane did not exceed ± 0.5 and ± 0.1 mm in the streamwise and radial directions, respectively.

The gas for the jet was supplied from pressurized tanks and was filtered to remove oil, moisture, and particulates. Furthermore, a long supply line with several looped copper sections ensured that the issuing gas was in temperature equilibrium with the ambient air. A 100-l/min mass flow controller, accurate to $\pm 1\%$ of full scale and with repeatability of $\pm 0.2\%$ of full scale per manufacturer's specifications, was used to meter the gas. Calibration of the mass flow controller was performed for each gas using an Optiflow 730 Digital Flowmeter. The uncertainty in the mass flow calibration was less than $\pm 1.5\%$. Ambient conditions, temperature, and barometric pressure were recorded at the beginning and end of each complete test (generally lasting 2–3 h) for determining the average gas properties. Overall, beginning-to-end ambient variations were small, less than $\pm 0.5^\circ$C and ± 2 Pa.

To accurately evaluate the effect of flow conditions at discharge on jet development, the velocity distribution at the exit of the jet was mapped out as a function of Reynolds number. Because this distribution for a particular Reynolds number is independent of the gas makeup in the present setup, air was used as the working fluid to facilitate measurements of the exit profile with a hot-wire probe. These measurements were done before moving the pipe assembly into the RLSF. A 2.5-μm-diam tungsten wire hot-wire probe, with a sensing length of 0.4 mm, was used. It was mounted on a two-dimensional computer-controlled traverse. The wire was centered longitudinally along a jet diameter and traversed perpendicular to it with the wire's longitudinal axis perpendicular to the travel and flow directions. Full traverses along the diametral direction were made at a streamwise station of 0.5 mm from the exit plane. The error in initially positioning the probe was less than ± 0.05 and ± 0.1 mm in the radial and streamwise directions, respectively. Subsequent positioning was done at a manufacturer's specified accuracy of ± 1.6 and ± 3.2 μm, respectively.

The hot-wire probe was controlled by a TSI IFA100 anemometer, which incorporated voltage gain and offset capabilities for optimizing the signal output over the voltage range of the analog-to-digital converter. Calibration of the hot wire was performed using a TSI Model 1125 Calibrator unit over the velocity range of 2–60 m/s. The calibration data were fitted to a general King's law relation, $E^2 = A + BU^n$, where E is the hot-wire voltage output and A, B, and n are calibration constants. In the experiment, U was determined from the hot-wire output signal via the calibration curve, and the absolute error was estimated to be approximately 3%. The square wave frequency response of the hot wire was 25 kHz. Data sampling was performed at 2 and 10 kHz and with 20,000 and 30,000 samples, respectively. The high sampling rate was used to better evaluate velocity dynamics along the centerline. The uncertainty associated with determining the mean and rms values was less than 0.5% of the initial mean centerline value at the exit of the jet.

Results

A. Exit Conditions

Radial profiles of the normalized mean velocity, turbulence intensity, skewness, and flatness for the air jet at $z/r_0 = 0.16$ are shown in Fig. 1. Integration of the mean velocity profile gives the ratio of bulk-to-centerline (maximum) velocity as a function of Reynolds number shown in Fig. 2 (Refs. 24 and 25), which was within 1–2% of the same ratio obtained by calculating the bulk velocity from the mass flow controller output. The resulting values for this ratio agree with previous measurements of fully developed flow in pipes and indicate that the flow is fully developed and turbulent at the exit of the pipe. The distributions for the turbulence intensity and high-order moments shown in Fig. 1 also agree well with fully developed pipe flow profiles in the same Reynolds-number range as reported by Lekakis et al.[26]

Normalized mean velocity profiles are observed to change little as the Reynolds number increases, for the range of Reynolds numbers studied here, reaching an asymptotic state (within experimental uncertainty) at $Re \approx 1.4 \times 10^4$. However, early investigations conducted by Nikuradse[17] and Laufer[27] show that the profile characteristics continue to change even to Reynolds numbers of $Re \approx 1 \times 10^9$, as reported by the former, a variation that is also reflected in the Moody chart depicting the skin-friction characteristics of commercially smooth pipes (Ref. 28, pp. 615–626). Aside from the Reynolds number, the Moody chart makes apparent that pipe roughness is another factor affecting final flow development

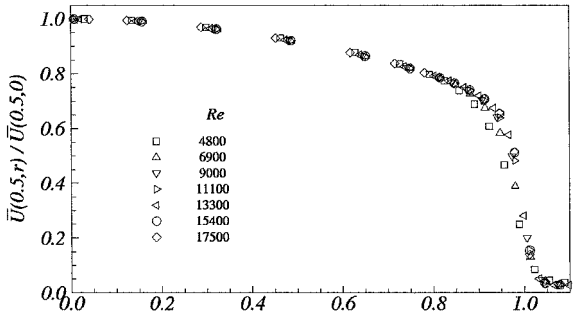

Normalized mean velocity

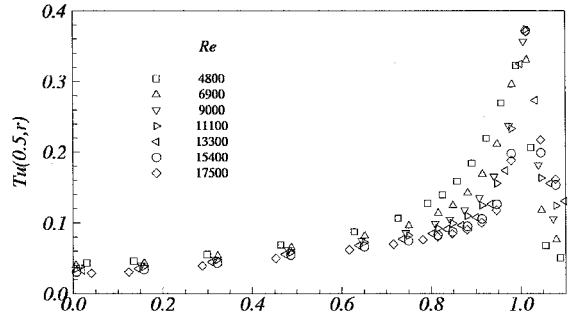

Turbulence intensity

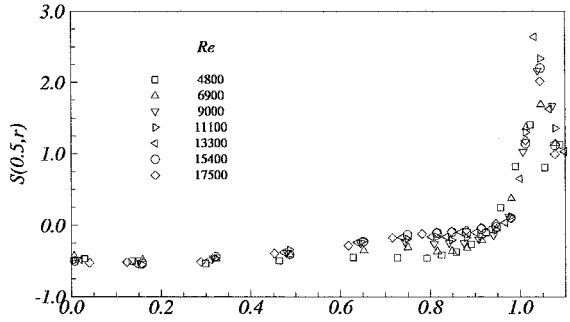

Skewness

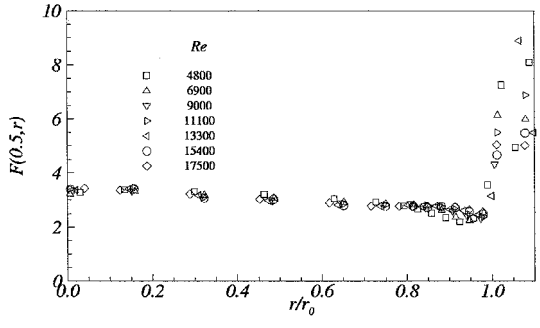

Flatness

Fig. 1 Velocity profile characteristics at $z/r_0 = 0.16$.

in pipes, but for commercially smooth pipes these effects are negligible in the range of low to moderately high Reynolds numbers. Furthermore, the relative variation of the velocity profile characteristics is most significant in the early range of Reynolds numbers, and it is in this range that significant Reynolds-number effects on the centerline decay of turbulent jets are observed.

The relative variation of the turbulence intensity distribution appears to change more significantly with Reynolds numbers in comparison to the normalized mean velocity and does not reach an asymptotic state in the range of Reynolds numbers investigated. Integrating the distribution and normalizing by the cross-sectional area of the jet exit yield the turbulence intensity flux per unit area τ_0 shown in Fig. 3 (Refs. 26 and 29–32). Comparison of the present results with similar data reported in the literature is good. Significant pipe roughness is expected to effect the value of τ_0 because it is known from the Moody chart that skin-friction characteristics

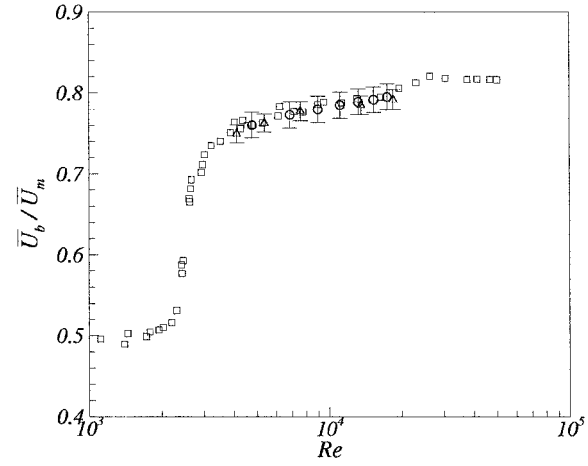

Fig. 2 Bulk-to-centerline velocity ratio variation with Reynolds number for fully developed pipe flow: ○, present measurements (at discharge); □, Ref. 24 (within pipe); and △, Ref. 25 (within pipe and at discharge).

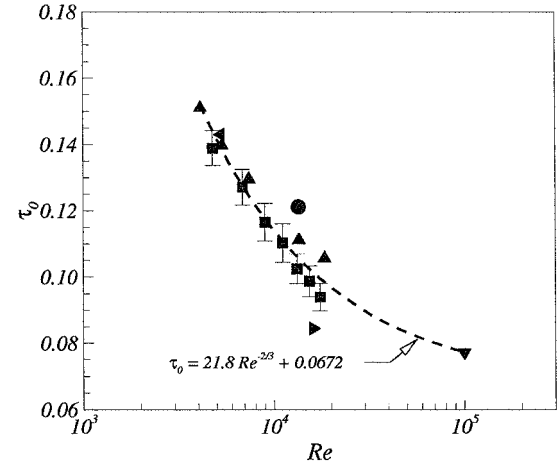

Fig. 3 Turbulence intensity flux per unit area for fully developed pipe flow conditions: ■, present measurements (at discharge); ▲, Ref. 26 (within pipe); ▼, Ref. 29 (within pipe); ▶, Ref. 30 (at discharge); ◀, Ref. 31 (within pipe); ●, Ref. 32 (at discharge); and – – –, best fit.

(which correlate to velocity profile characteristics) are a function of the pipe roughness as well as Reynolds number. The data shown in Fig. 3 may be categorized as being for commercially smooth pipes, and for the moderately high Reynolds numbers considered, mild variations in surface roughness are expected to have a negligible effect. It appears that an asymptotic state is attainable at a high Reynolds number, and fitting the data accordingly gives the result shown in the figure. Note that this fit is an estimate, and an expanded detailed investigation is necessary to accurately evaluate the variation of τ_0 with Reynolds numbers and perhaps with pipe roughness as well. Nevertheless, the data shown cover a range of Reynolds numbers in which the relative variation of τ_0 is greatest, and as mentioned earlier, it is in this range that significant Reynolds-number effects on the centerline decay of turbulent jets are observed.

B. Centerline Velocity: Air Jet

Distributions of mean centerline velocity normalized by the value at the exit are shown in Fig. 4 and compared with similar data reported by Lee et al.[33] The agreement is good, and the data clearly indicate an asymptotic collapse of the decay curves as the Reynolds number increases. The streamwise distance has been normalized by the effective radius in an attempt to perhaps capture the effect of the mean velocity profile variation with Reynolds numbers. Although the effective radius concept has been more widely used to capture variable density effects, its use in Fig. 4 for normalizing the streamwise distance is appropriate because as defined in Eq. (3) the

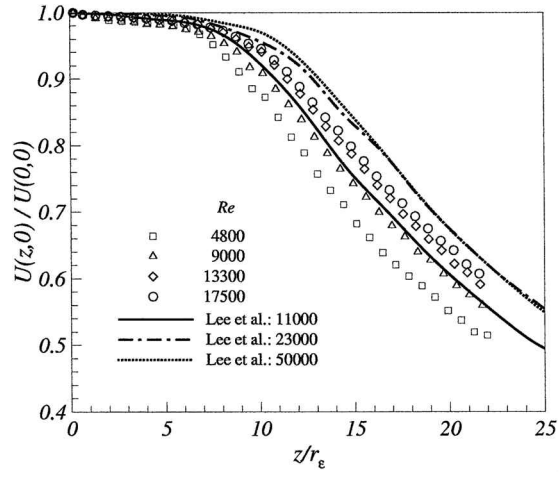

Fig. 4 Distributions of normalized mean centerline velocity in the near field of the air jet: streamwise location normalized by the effective radius. Symbols denote present measurements; lines denote data from Ref. 33.

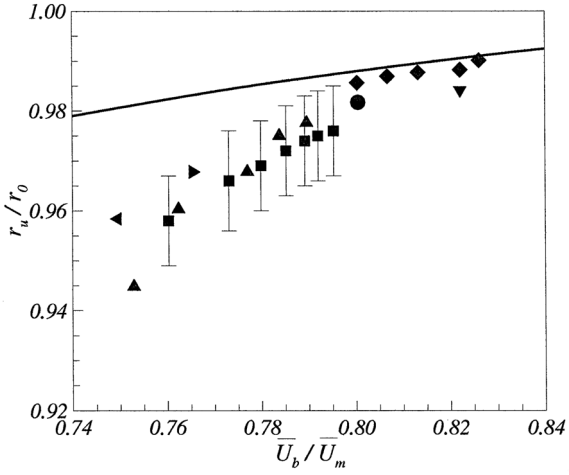

Fig. 5 Adjusted jet exit radius resulting from the nonuniform velocity distribution of fully developed turbulent flow: ■, present measurements (at discharge); ▲, Ref. 26 (within pipe); ▼, Ref. 29 (within pipe); ▶, Ref. 30 (at discharge); ◀, Ref. 31 (within pipe); ♦, Ref. 17 (within pipe); ●, Ref. 34 (at discharge); and ——, power law profile.

effective radius incorporates the shape of the initial velocity profile through the mass and momentum fluxes. Because the density at the exit of the jet is constant across the pipe, the effective radius can be rewritten as

$$r_\varepsilon = R_\rho^{\frac{1}{2}} r_u, \qquad \text{with} \qquad r_u = \frac{M_0}{(\pi N_0)^{\frac{1}{2}}} \tag{6}$$

to decouple effects of density from those due to the nonuniform initial velocity profile. In Eq. (6),

$$M_0 = \int_{A_0} U(0,r)\,\mathrm{d}A, \qquad N_0 = \int_{A_0} U^2(0,r)\,\mathrm{d}A$$

For a uniform (top-hat) velocity profile $r_u = r_0$, whereas for a parabolic profile $r_u = \sqrt{3}r_0/2$. Because the velocity profile changes with Reynolds numbers for fully turbulent flow, r_u in this case needs to be determined from the experimental data. The present results are shown in Fig. 5 along with other data obtained from the literature (Refs. 17, 29–31, and 34), and the resulting curve if one assumes a power law shape for the turbulent profile

$$\frac{\bar{U}(0,r)}{\bar{U}(0,0)} = \left(1 - \frac{r}{r_0}\right)^{1/\kappa} \tag{7}$$

where κ takes on values of 5–7 depending on the Reynolds number (see Ref. 28, pp. 596–600). The relative adjustment due to mean velocity profile shape changes is quite small (less than 1%) and therefore does not explain the large Reynolds number effect observed in the near field.

On the other hand, turbulence intensity profiles (Fig. 1) and the corresponding turbulence flux per unit area (Fig. 3) show a significant variation with Reynolds numbers. It appears that this variation correlates negatively with the apparent shift of the velocity decay curves (Fig. 4), namely, a high τ_0 (low Reynolds number) is linked to an earlier decay, whereas a low τ_0 (high Reynolds number) is linked to a later decay. Furthermore, values of τ_0 appear to approach an asymptotic state as the Reynolds number increases. This asymptotic behavior is most interesting because it correlates well with a similar state reached by the jet centerline velocity decay curves, indicating that at high Reynolds numbers, when $\tau_0 \approx$ const, the act of increasing the initial momentum of the initially turbulent jet does little, if anything, toward changing the centerline velocity decay. This implies that the initial turbulence intensity may be responsible for the shift in the velocity distribution observed in the near field. After all, in the present configuration the initial turbulence intensity is a significant source of excitation that feeds into the growing shear layer, thus governing directly the growth of turbulence responsible for breaking up the jet potential core. As a result, levels of initial turbulence intensity that are higher than the asymptotic value can lead to the upstream shift of the centerline velocity distribution observed at low Reynolds numbers. It should then be possible to capture this effect by introducing an appropriate scale that incorporates the relative magnitude of the perturbation to the flow due to the initial turbulence intensity.

One way to achieve this, which is the result of the present investigation, is to modify the effective radius (thus also taking into account mean velocity distribution changes) by factoring in the initial turbulence intensity flux per unit area in its definition to yield a new length scale,

$$r_0^* = R_\rho^{\frac{1}{2}} r_u \tau_0^{-\frac{1}{2}} = \frac{R_\rho^{\frac{1}{2}} M_0}{(\pi N_0 \tau_0)^{\frac{1}{2}}} \tag{8}$$

Using the preceding length scale to normalize the streamwise distance variable in the centerline velocity distributions of Fig. 4 effectively collapses the curves, as shown in Fig. 6. The Reynolds number effect on the centerline time-averaged growth rate and the resulting virtual origin shift has been effectively scaled. Extension of the normalization into the far field fails as expected (Fig. 7) because memory of the initial flow structure is incorporated into Eq. (8). Once the flow attains the self-similar state, the dimensional analysis performed by Dahm and Dimotakis[13] indicates that Eq. (6) is the proper length scale for normalization.

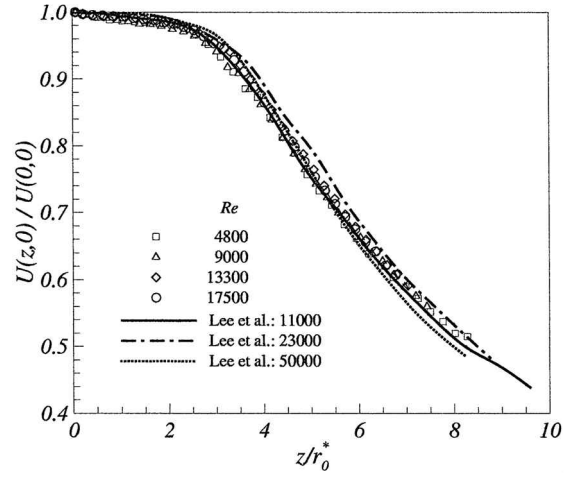

Fig. 6 Distributions of normalized mean centerline velocity in the near field of the air jet: streamwise location normalized by length scale incorporating initial turbulence intensity flux information, as well as mass and momentum. Symbols denote present measurements; lines denote data from Ref. 33.

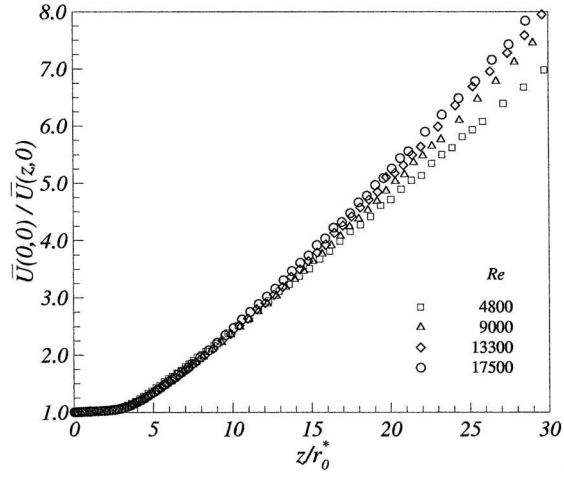

Fig. 7 Inverse decay of mean centerline velocity in the near and far fields of the air jet.

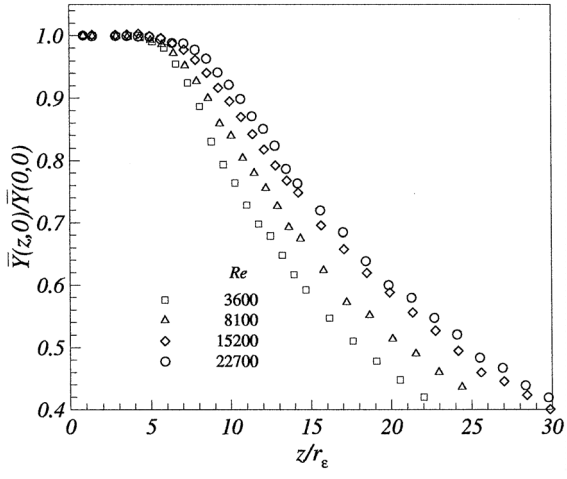

Fig. 8 Mean mass fraction of propane concentration along the centerline; streamwise location normalized by the effective radius.

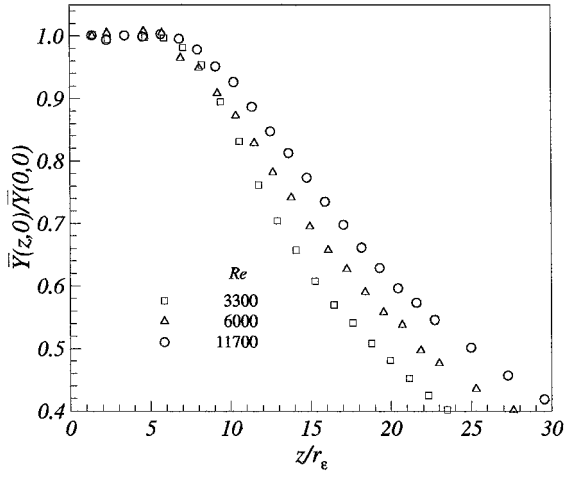

Fig. 9 Mean mass fraction of methane concentration along the centerline; streamwise location normalized by the effective radius.

C. Centerline Concentration

Near-field evolution of the concentration scalar is primarily governed by the evolution of the velocity field. Consequently, the initial turbulence intensity is expected to play an equivalent role in the diffusion of the scalar as it did for the velocity field. In Figs. 8–11 the results from the RLS measurements are shown. Figures 8 and 9 show the streamwise mean mass fraction decay for the propane and methane jet configurations, respectively, for various Reynolds numbers and with the streamwise distance normalized by r_ε. The

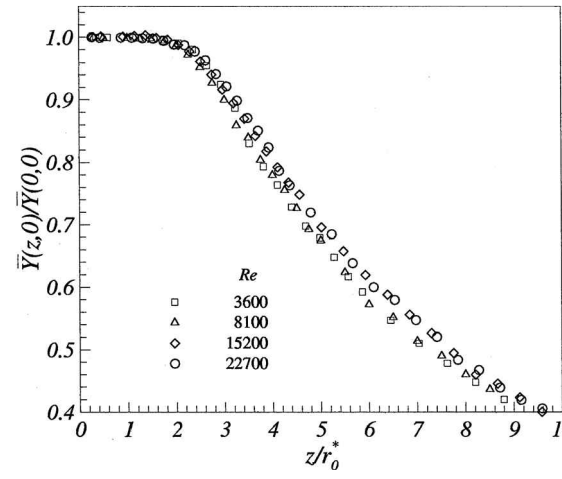

Fig. 10 Mean mass fraction of propane concentration along the centerline; streamwise location normalized by the proposed length scale.

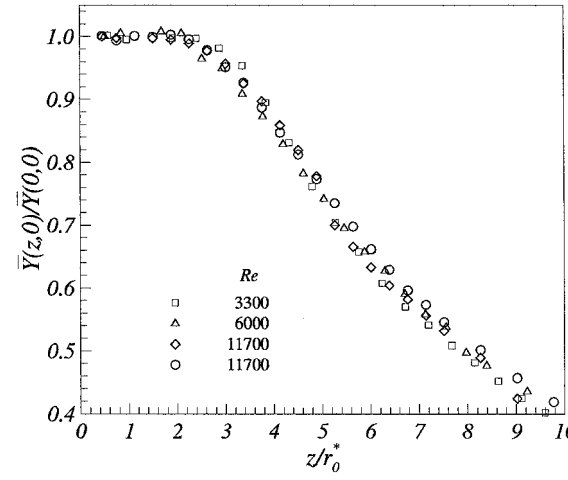

Fig. 11 Mean mass fraction of methane concentration along the centerline; streamwise location normalized by the proposed length scale.

downstream shift of the virtual origin with increasing Reynolds numbers is clearly apparent.

Although velocity measurements at the exit of the propane and methane jets were not made, the initial velocity profile information gathered for the air jet can be used appropriately. Doing so yields values for the turbulence intensity flux per unit area that correspond to the Reynolds numbers of the propane and methane jets (obtained by fitting the data in Fig. 3). Thus, a new length scale may be determined according to Eq. (8), as was done for the velocity field in the air jet. Using this length to rescale the mean mass fraction distribution yields good results for the centerline development in the near field, as shown in Figs. 10 and 11.

The scaling of the near-field velocity and concentration centerline distributions using r_0^* results in a generic curve for each case. A comparison between the decay curve of the velocity and concentration fields may be made through this generic curve, as shown in Fig. 12. The results in the figure support the general consensus that the scalar field evolves faster than the velocity field. Also, the disagreement between the propane and methane curves indicates that local scaling of the density ratio needs to be incorporated into r_0^* because in the near field the effective jet density cannot be approximated by the ambient density, as is the case in the far field. This idea has been recently proposed by Sautet and Stepowski[35] and Stepowski and Sautet[36] with regard to the effective radius definition.

Further Discussion

The definition of the effective radius [Eqs. (3) and (6)] incorporates information about the initial state of the mean flow, specifically the relative adjustment to the actual radius as a result of deviations

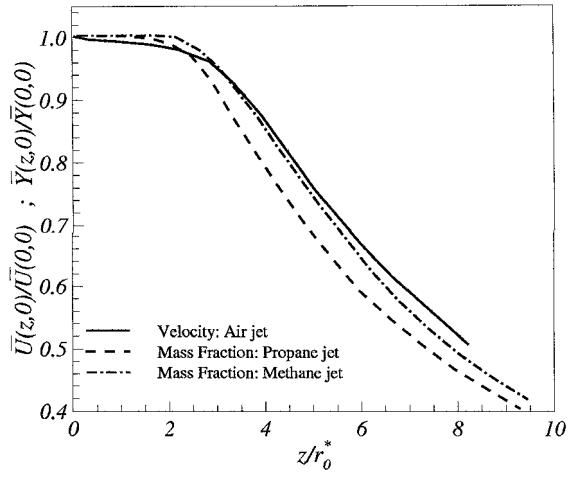

Fig. 12 Comparison of generic velocity and concentration centerline decay curves.

from the ideal case of the uniform initial distribution. At the final state of development (far-field region), jet characteristics assume similar radial distributions, which are markedly different from the initial distributions at the jet exit. Therefore, mean velocity and concentration distributions undergo a certain degree of shape alteration in the near field of the jet, the extent of which may inversely correlate with jet spreading rate characteristics. In his investigation of the pressure losses past sudden expansions and contractions, Kays[37] introduced factors, similar to M_0 and N_0 in Eq. (6), to successfully correct for the realistic condition of nonuniform velocity distributions at the inlet and outlet to the system. Jet development may also be correlated using such factors, and the use of r_ε to form the basis for the new proposed length scale has roots in the preceding observation. Under fully developed turbulent conditions, however, initial mean velocity profile variations with Reynolds numbers are found to be minor, and as the present results indicate, another characteristic of the velocity profile is influencing near-field development.

The introduction of factors to correct for nonuniform velocity distribution effects has so far involved only the mean characteristics. For turbulent flows, however, the inclusion of fluctuating velocity effects in the definition of a scale is clearly necessary to fully capture the effects of initial conditions on flow development. If the velocity terms in the mass and momentum flux terms of Eq. (3) are separated into mean and fluctuating components and subsequently time averaged, then an additional term multiplying the mean momentum flux term is apparent. This term is a function of the local turbulence intensity, and although not exactly equivalent to τ_0, it supports the general form of the new length scale r_0^*.

Russ and Strykowski[38] indicated that the instability mechanisms responsible for periodic concentrations of vorticity (formation of large-scale structures) in initially laminar shear layers (or low-turbulence-level nozzle flows) are bypassed when turbulent conditions exist. The broadband nature of turbulence is cited for disrupting vortex formation and pairing processes responsible for elevated momentum mixing under initially laminar conditions.[39,40] The loss of large-scale structures as a mechanism for the initial redistribution of momentum renders amplification of broadband turbulence as the only significant mechanism for the initial growth of turbulence in the shear layer, in the absence of other artificial excitation sources. Hence, the magnitude of the turbulence intensity at the jet exit might be expected to determine the changes in the growth of turbulence accompanying the development of such flows. However, due to the nonlinear nature of the equations of motion, any initial excitation of the shear layer is expected to propagate in a nonlinear fashion, cascading into a series of disturbances that further amplify the local fluctuations. The success of r_0^* in effectively scaling the observed Reynolds-number dependencies in the near field indicates that this hypothesis is correct.

The present results demonstrate the importance of initial conditions on jet mixing processes. From an engineering point of view the scaling reported in this paper is valuable because it is based solely on the initial conditions and not on an empirical formulation. The scaling becomes less robust far from the exit of the jet, emphasizing the decreasing effect of initial conditions. Capturing this decreasing effect may be possible by defining a dynamic length scale that incorporates the local turbulence intensity information in a way such that this contribution decays to zero as the far-field similarity region is approached. This is similar to the idea of replacing the ambient density with a local average density, as proposed by Sautet and Stepowski[35] and Stepowski and Sautet.[36]

Conclusions

Centerline velocity and concentration data were presented for axisymmetric jets having initially fully developed turbulent conditions showing the effect of Reynolds number on near-field development that is commonly reported in the literature. A careful investigation of the initial velocity distribution just downstream of the exit plane revealed that the initial turbulence intensity distribution is the major source for this apparent Reynolds-number dependence.

The effective radius previously used to nondimensionalize the streamwise displacement variable in the far field of jets was used as a basis to create a new length scale that also incorporates the initial turbulence intensity flux per unit area. Subsequent scaling of the mean velocity and mean mass fraction distributions along the centerline of the jet resulted in the effective collapse of the individual fields for all of the Reynolds numbers investigated. This implies that Reynolds-number independence in the near field of initially turbulent jets is possible by normalizing the streamwise displacement variable with a length scale that incorporates the initial mass, momentum, and turbulence intensity flux information. Analysis of the fluctuating velocity and concentration fields is currently under way, as is the extension to other geometries such as flow exiting a contoured nozzle. The important outcome of this work is expected to be an effective procedure for predicting the location of the virtual origin in axisymmetric jets having a wide range of initial conditions.

Acknowledgment

The authors are grateful to I. Lekakis for providing his pipe flow profile data.

References

[1]Harsha, P. T., "Free Turbulent Mixing: A Critical Evaluation of Theory and Experiment," Arnold Engineering Development Center, AED-TR-71-36, Arnold Air Force Station, TN, Feb. 1971.

[2]Chen, C. J., and Rodi, W., *Vertical Turbulent Buoyant Jets—A Review of Experimental Data*, Pergamon, New York, 1980.

[3]Gouldin, F. C., Schefer, R. W., Johnson, S. C., and Kollmann, W., "Nonreacting Turbulent Mixing Flows," *Progress in Energy and Combustion Science*, Vol. 12, 1986, pp. 257–303.

[4]Townsend, A. A., *The Structure of Turbulent Shear Flow*, 2nd ed., Cambridge Univ. Press, London, 1976.

[5]Wygnanski, I., and Fiedler, H., "Some Measurements in the Self-Preserving Jet," *Journal of Fluid Mechanics*, Vol. 38, 1969, pp. 577–612.

[6]Thring, M. W., and Newby, M. P., "Combustion Length of Enclosed Turbulent Jet Flames," *Fourth (International) Symposium on Combustion*, Williams and Wilkins Co., Pittsburgh, PA, 1953, pp. 789–796.

[7]Becher, H. A., Hottel, H. C., and Williams, G. C., "The Nozzle-Fluid Concentration Field of the Round, Turbulent, Free Jet," *Journal of Fluid Mechanics*, Vol. 30, Pt. 2, 1967, pp. 285–303.

[8]Avery, J. F., and Faeth, G. M., "Combustion of a Submerged Gaseous Oxidizer Jet in a Liquid Metal," *Fifteenth (International) Symposium on Combustion*, Combustion Inst., Pittsburgh, PA, 1975, pp. 501–512.

[9]Dahm, W. A., and Dimotakis, P. E., "Measurements of Entrainment and Mixing in Turbulent Jets," *AIAA Journal*, Vol. 25, No. 9, 1987, pp. 1216–1223.

[10]Dowling, D. R., and Dimotakis, P. E., "Similarity of the Concentration Field of Gas-Phase Turbulent Jets," *Journal of Fluid Mechanics*, Vol. 218, 1990, pp. 109–141.

[11]Pitts, W. M., "Effects of Global Density Ratio on the Centerline Mixing Behavior of Axisymmetric Turbulent Jets," *Experiments in Fluids*, Vol. 11, 1991, pp. 125–134.

[12]Richards, C. D., and Pitts, W. M., "Global Density Effects on the Self-Preservation Behaviour of Turbulent Free Jets," *Journal of Fluid Mechanics*, Vol. 254, 1993, pp. 417–435.

[13]Dahm, W. A., and Dimotakis, P. E., "Mixing at Large Schmidt Number in the Self-Similar Far Field of Turbulent Jets," *Journal of Fluid Mechanics*, Vol. 217, 1990, pp. 299–330.

[14]Pitts, W. M., "Reynolds Number Effects on the Mixing Behavior of Axisymmetric Turbulent Jets," *Experiments in Fluids*, Vol. 11, 1991, pp. 135–141.

[15]Patel, R. P., "A Note on Fully Developed Turbulent Flow down a Circular Pipe," *Aeronautical Journal*, Feb./March 1974, pp. 93–97.

[16]Papadopoulos, G., and Durst, F., "Influence of Tripping Level and Development Length on Pipe Flow Discharge Characteristics," AIAA Paper 97-0552, Jan. 1997.

[17]Nikuradse, J., "Gesetzmäßigkeiten der turbulenten Strömung in glatten Rohren," Forshchungsheft 357, Beilage zu Forschung auf dem Gebeite des Ingenieurwesens, VDI-Verlag, G. M. G. H., Berlin, 1932.

[18]Durst, F., Kikura, H., Lekakis, I., Jovanovíc, J., and Ye, Q., "Wall Shear Stress Determination from Near-Wall Mean Velocity Data in Turbulent Pipe and Channel Flows," *Experiments in Fluids*, Vol. 20, 1996, pp. 417–428.

[19]Ebrahimi, I., "Axialer Verlauf der Geschwindigkeit in Luft-Freistrahlen," *Forschung im Ingenieurwesen*, Vol. 42, 1976, pp. 33–35.

[20]Ebrahimi, L., and Kleine, R., "Konzentrationsfelder in isothermen Luft-Freistrahlen," *Forschung im Ingenieurwesen*, Vol. 43, 1977, pp. 25–30.

[21]Lenze, B., "Der Einfluss der Reynoldszahl auf den Verlauf der Geschwindigkeiten und Konzentrationen von Freistrahlen unterschiedlicher Dichte," *Forschung im Ingenieurwesen*, Vol. 42, 1976, pp. 184–186.

[22]Bryner, N., Richards, C. D., and Pitts, W. M., "A Rayleigh Light Scattering Facility for the Investigation of Free Jets and Plumes," *Review of Scientific Instruments*, Vol. 63, 1992, pp. 3629–3635.

[23]Pitts, W. M., and Kashiwagi, T., "The Application of Laser-Induced Rayleigh Light Scattering to the Study of Turbulent Mixing," *Journal of Fluid Mechanics*, Vol. 141, 1984, pp. 391–429.

[24]Patel, V. C., and Head, M. R., "Some Observations on Skin Friction and Velocity Profiles in Fully Developed Pipe and Channel Flows," *Journal of Fluid Mechanics*, Vol. 38, Pt. 1, 1969, pp. 181–201.

[25]Papadopoulos, G., Lekakis, I., and Durst, F., "Reynolds Number Asymptotic Covariance for Turbulent Pipe Flow Past a Sudden Expansion," American Society of Mechanical Engineers, ASME Paper FEDSM97-3323, Vancouver, BC, Canada, June 1997.

[26]Lekakis, I., Durst, F., and Sender, J., "LDA Measurements in the Near-Wall Region of an Axisymmetric Sudden Expansion," *7th International Symposium on Applications of Laser Techniques to Fluid Mechanics* (Lisbon, Portugal), 1994.

[27]Laufer, J., "The Structure of Turbulence in Fully Developed Pipe Flow," National Bureau of Standards, Rept. 1174, Washington, DC, Oct. 1952.

[28]Schlichting, H., *Boundary-Layer Theory*, 7th ed., McGraw–Hill, New York, 1979.

[29]Yeh, T. T., and Mattingly, G. E., "Pipeflow Downstream of a Reducer and Its Effects on Flowmeters," *Flow Measurement and Instrumentation*, Vol. 5, 1994, pp. 181–187.

[30]Gladnick, P. G., Enotiadis, A. C., LaRue, J. C., and Samuelsen, G. S., "Near-Field Characteristics of a Turbulent Coflowing Jet," *AIAA Journal*, Vol. 28, 1990, pp. 1405–1414.

[31]Eggels, J. G. M., Westerweel, J., and Nieuwstadt, F. T. M., "Direct Numerical Simulation of Turbulent Pipe Flow," *Applied Science Research*, Vol. 51, 1993, pp. 319–324.

[32]Vradis, G. C., Ötügen, M. V., Kim, S. W., and Kim, D. B., "Round Incompressible Jets with Asymmetric Initial Velocity Distributions," *AIAA Journal*, Vol. 31, 1993, pp. 814, 815.

[33]Lee, D. H., Chung, Y. S., and Kim, D. S., "Surface Curvature Effects on Flow and Heat Transfer from a Round Impinging Jet," *31st ASME National Heat Transfer Conference*, HTD-Vol. 324, American Society of Mechanical Engineers, 1996, pp. 73–83.

[34]Ferdman, E., Otugen, M. V., and Kim, S., "Effect of Initial Velocity Profile on the Development of Round Jets," *Journal of Propulsion and Power* (submitted for publication).

[35]Sautet, J. C., and Stepowski, D., "Dynamic Behavior of Variable-Density, Turbulent Jets in Their Near Development Fields," *Physics of Fluids*, Vol. 7, No. 11, 1995, pp. 2796–2806.

[36]Stepowski, D., and Sautet, J. C., "Axial Decay of Unmixedness in Round Turbulent Jets with Variable Density," *IUTAM Symposium on Variable Density Low Speed Turbulent Flows* (Marseille, France), 1996, pp. 151–153.

[37]Kays, W. M., "Loss Coefficients for Abrupt Changes in Flow Cross Section with Low Reynolds Number Flow in Single and Multiple-Tube Systems," *Transactions of the American Society of Mechanical Engineers*, Vol. 72, 1950, pp. 1067–1074.

[38]Russ, S., and Strykowski, P. J., "Turbulent Structure and Entrainment in Heated Jets: The Effect of Initial Conditions," *Physics of Fluids A*, Vol. 5, No. 12, 1993, pp. 3216–3225.

[39]Winant, C. D., and Browand, F. K., "Vortex Pairing, the Mechanism of Turbulent Mixing-Layer Growth at Moderate Reynolds Numbers," *Journal of Fluid Mechanics*, Vol. 63, 1974, pp. 237–255.

[40]Drubka, R. E., Reisenthel, P., and Nagib, H. M., "The Dynamics of Low Initial Disturbance Turbulent Jets," *Physics of Fluids A*, Vol. 1, 1989, pp. 1723–1735.

G. M. Faeth
Editor-in-Chief